Journal of Solid Mechanics Vol. 6, No. 3 (2014) pp. 278-288

Energy-Based Prediction of Low-Cycle Fatigue Life of CK45 Steel and SS316 Stainless Steel

M. Shariati[1,*], H. Mehrabi[2]

[1]*Department of Mechanical Engineering, Ferdowsi University of Mashhad, Mashhad, Iran*
[2]*Department of Mechanical Engineering, Shahrood University of Technology, Shahrood, Iran*

Received 9 April 2014; accepted 12 June 2014

ABSTRACT

In this paper, low cycle fatigue life of CK45 steel and SS316 stainless steel under strain-controlled loading are experimentally investigated. In addition, the impact of mean strain and strain amplitude on the fatigue life and cyclic behavior of the materials are studied. Furthermore, it is attempted to predict fatigue life using energy and SWT damage parameters. The experimental results demonstrate that increase in strain amplitude decreases fatigue life for both materials, strain amplitude has a remarkable effect on fatigue life, and the impact of mean strain is approximately negligible. Furthermore, the energy damage parameter provides more accurate prediction of fatigue life for both materials.

Keywords: Low cycle fatigue; Damage parameter; CK45 steel; SS316 stainless steel; Cyclic behavior

1 INTRODUCTION

ENGINEERING structures are mostly under cyclic loadings. By the time loadings enter plastic regime low cyclic fatigue phenomena take on added importance in designing the structures. Several studies have been conducted to investigate and predict low cycle fatigue life of different materials. Yang [1] studied low cycle fatigue life of CK45 steel in both strain-control and stress-control states and investigated the impact of strain amplitude and mean strain. Date et al. [2] surveyed low cycle fatigue life of SS316FR steel under strain-control loading along with variable mean strain, and the impact of ratcheting on the fatigue life. Moreover, several studies have been executed for predicting low cycle fatigue life based on different models. In general, these models can be divided into two categories [3,4] : equivalent strain/stress models and energy and work models.

The most applicable strain/stress based model is Coffin-Manson's. Several researchers have used this method or its optimized versions [5-7]. Energy-based models have also been employed by a number of researchers to predict the fatigue life and to determine fatigue damage parameter for different types of steel and other materials. Halford [8], based on plastic energy, attempted to analyze low cycle fatigue life of steels. Ellyin and Kujawski [9] offered an energy criterion for predicting the fatigue life of different types of steel. Golos and Ellyin [10] developed a theory for fatigue parameter, based on the total strain energy. Sugiura et al. [11] provided a model for estimating low fatigue strength cycle of structural steel under multi-axial and non-proportional loading. In addition, a number of studies have been performed to determine the low cycle fatigue life based on energy model for some types of materials, such as 316 stainless steel [12], 2.25 Cr-lMo steel [13], extruded magnesium alloy [14], BS 460B and Bs

* Corresponding author. Tel.: +98 9121733750.
E-mail address: mshariati44@um.ac.ir (M. Shariati).

500B steel bars [15], TiAl alloys [16] and high-strength structural steel [17]. In these studies, fatigue life prediction has been done carefully based on energy method. Energy-method has not been used yet to predict the fatigue life of CK45 steel and SS316 stainless steel. Additionally, the SWT damage parameter is compared with the energy damage parameter, in this study.

The purpose of this survey is to investigate the fatigue life of two applicable steels in industry, CK45 steel and SS316 stainless steel, under uniaxial cyclic loading in strain-control mode. In addition, the impact of strain amplitude and mean strain parameters on the fatigue life and cyclic behavior of the material is studied. At the end, the energy and SWT damage parameters were analyzed and compared to experimental results.

2 GEOMETRY AND MECHANICAL PROPERTIES OF THE MATERIAL

The specimens of fatigue experiments are considered in form of bars with gauge length of 30mm and diameter of 10mm (Fig. 1). The simple tensile test was conducted on these specimens using a servo-hydraulic fatigue testing system (INSTRON 8802) at 0.01 mm/s displacement rate to determine tensile properties in room temperature. The result is shown in Figs. 2 and 3. From Fig. 2 and 3 some basic mechanical properties could be measured such as yield strength, tensile strength, Young's modulus and elongation. The measured values for both CK45 steel and SS316 stainless steel are listed in Table 1. It is worth mentioning that in order to improve the measurement accuracy, an extensometer was used at the middle of the specimens during experiments.

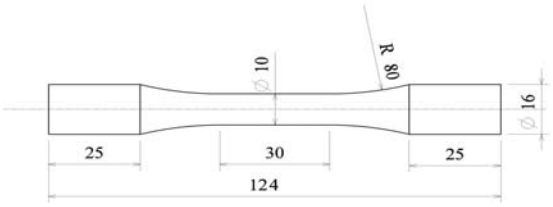

Fig. 1
Geometric dimensions of the specimens (mm).

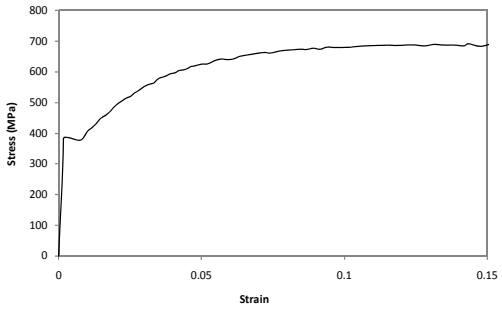

Fig. 2
Monotonic tensile stress-strain curve for CK45 steel.

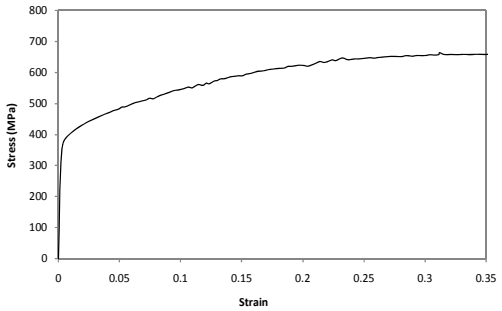

Fig. 3
Monotonic tensile stress-strain curve for SS316 stainless steel.

Table 1
Mechanical properties of CK45 steel and SS316 stainless steel

Material	Yield strength (MPa)	Tensile strength (MPa)	Young's modulus (GPa)	Uniform elongation (%)
CK45	384	690	204	15
SS316	372	658	193	35

3 EXPERIMENTAL RESULTS AND DISCUSSION

The purpose of strain-control tests is to investigate the cyclic behavior and predict the fatigue life of present materials based on energy and SWT parameters. All fatigue tests were performed using servo hydraulic fatigue testing system (INSTRON 8802) under uniaxial cyclic loadings. In addition, the tests have been conducted at 10Hz frequency. The servo hydraulic machine and the way they are placed in the machine are presented in Fig. 4.

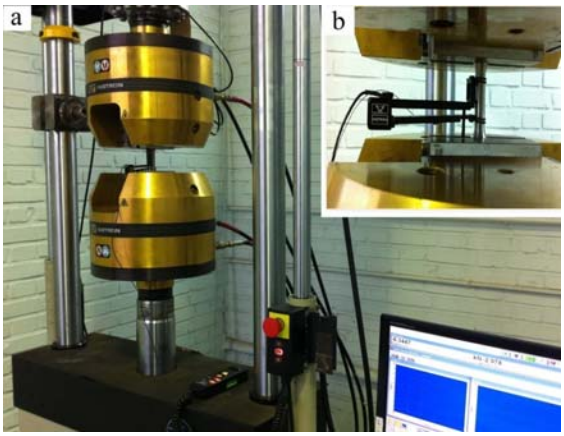

Fig. 4
(a) Servo-hydraulic fatigue testing system (INSTRON 8802); (b) Close view of how the specimen is placed between the jaws and connected to the extensometer.

3.1 Investigating the cyclic behavior of the materials

Figs. 5 and 6 demonstrates the cyclic hardening/softening behavior of Ck45 steel and SS316 stainless steel, respectively. Form Fig. 5, it can be seen that for CK45 steel the cyclic behavior of the material at the strain amplitude of 0.83% presents a high softening feature in initial cycles. The material then shows a stable cyclic behavior. The cyclic behavior of the material varies by increasing the strain amplitude. In that, for strain amplitude of 1.25%, for a little number of cycles (about 15 cycles) a high cyclic hardening occurs. Then, a cyclic softening behavior occurs for approximately 200 cycles and a the material presents a slight hardening behavior up to the failure. From Fig. 6, it can be seen that for SS316 stainless steel the stress amplitude increases with a rapid rate at initial cycles and after that the material presents apparent cyclic softening behavior. It can be concluded from Fig. 6 that the cyclic softening/hardening behavior of SS316 stainless steel depends on strain amplitudes. When the strain amplitude is relatively larger (1.25%) the material shows a relatively higher softening behavior. Therefore, it can be concluded that for both materials, the cyclic softening/hardening features of materials are related to the strain amplitudes. Therefore, for CK45 steel the cyclic behavior of material in the larger strain amplitude tend to change from softening to hardening after several cycles. However, for SS316 stainless steel the cyclic behavior remains softening for two different strain amplitudes after the peak values and the cyclic behavior of the material tend to presents a relatively higher softening behavior for the larger strain amplitude. This difference between the cyclic behaviors of the two materials is caused by the different material features such as structural and metallurgical changes created in the material, which per se is a distinctive topic.

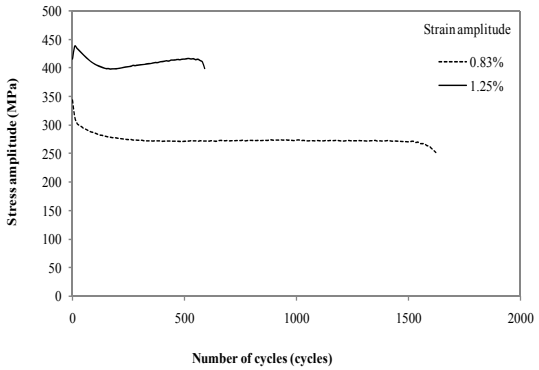

Fig. 5
Changes in stress amplitude to the number of cycles for symmetric strain-control loading for CK45 steel.

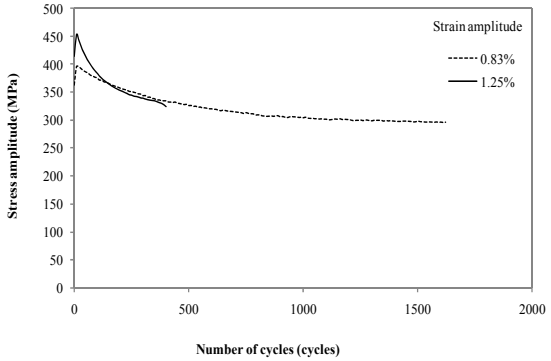

Fig. 6
Changes in stress amplitude to the number of cycles for symmetric strain-control loading for SS316 stainless steel.

3.2 Fatigue life

To study the effect of strain amplitude on the fatigue lives of the specimens, a number of experiments with constant mean strain and different stress amplitudes have been carried out. The mean strain and strain amplitude as well as the number of cycles to failure are listed in Table 2. It should be noted that the test numbers from C1 to C13 are related to CK45 steel specimens and the test numbers from S1 to S13 are related to SS316 stainless steel specimens. It is worth mentioning that the test numbers from C10 to C13 and S10 to S13 were performed in fully reversed condition, which means, the values of mean strains were considered to be zero. These tests were used to study the cyclic behavior of materials in order to avoid from the effects of relaxation, which usually occur under non-zero mean strain condition, and also to correlate the fatigue lives by using the energy damage parameter and SWT damage parameter. The energy damage parameter is based on the strain energy generated in cyclic loading and the SWT damage parameter is based on the Smith R.N., Watson P., and Topper, T.H. relationship [5] that includes both the cyclic strain range and the maximum stress, $\sigma_{max}\varepsilon_a$. This model, commonly referred to as the SWT parameter, was originally developed and continues to be used as a correction for mean stresses in uniaxial loading situations. The two damage parameters and their equations are given in Section 3.2.1 in order to predict the fatigue life.

Figs. 7 and 8 depict the fatigue lives of the specimens versus the strain amplitude at constant mean strain for both materials. As can be seen, for both materials the lives of the specimens decrease by increasing strain amplitude. This decreasing trend is almost equal for different mean strains and the mean strain has a slight impact on this trend. Hence, it can be concluded that the strain amplitude has a significant influence on fatigue life of specimens. Figs. 9 and 10 show the lives of the specimens to the mean strain at constant strain amplitude. As can be seen, the fatigue life is approximately remained constant by increasing mean strain and the effect of the mean strain on the lives of the specimens is almost ignorable for both materials. This behavior could be the result of quick relaxation and consequently, not remaining tensile mean stress during cyclic loading in order to decrease the fatigue life. From Fig. 9 it can be seen that the lives of the CK45 steel specimens are slightly increased by increasing the mean strain. However, from Fig. 10 it can be seen that the lives of the SS316 stainless steel specimens are slightly increased by increasing the mean strain till mean strain of 1.25% and for larger mean strains the fatigue lives are slightly decreased by increasing the mean strain.

Table 2
The results of strain-control fatigue test and strain and fatigue damage parameter values obtained for Ck45 steel and SS316 stainless steel

Test No.	$\varepsilon_{m\,(\%)}$	$\varepsilon_{a(\%)}$	$\Delta W_p(Mj/m^3)$	$\sigma_{max}\varepsilon_a(Mj/m^3)$	N_f(Cycles)
C1	1.66	1.66	10.63	7.02	330
C2	1.66	1.25	5.52	4.43	780
C3	1.66	0.83	1.90	2.44	4729
C4	1.25	1.66	10.42	6.94	332
C5	1.25	1.25	7.41	4.21	479
C6	1.25	0.83	1.99	2.50	4678
C7	0.83	1.66	11.53	6.81	300
C8	0.83	1.25	5.96	4.01	398
C9	0.83	0.83	2.04	2.36	4014
C10	0	1.66	11.89	6.65	220
C11	0	1.25	5.90	3.91	625
C12	0	0.83	3.02	2.21	1748
C13	0	0.62	2.16	1.53	6264
S1	1.66	1.66	11.78	6.68	203
S2	1.66	1.25	5.25	4.16	560
S3	1.66	0.83	2.12	2.21	5255
S4	1.25	1.66	10.32	5.42	240
S5	1.25	1.25	5.58	4.16	846
S6	1.25	0.83	1.65	2.20	5551
S7	0.83	1.66	12.12	6.29	187
S8	0.83	1.25	6.78	4.01	398
S9	0.83	0.83	2.04	2.09	3709
S10	0	1.66	11.92	7.12	220
S11	0	1.25	6.19	4.21	489
S12	0	0.83	2.37	2.37	2903
S13	0	0.62	1.86	1.65	6264

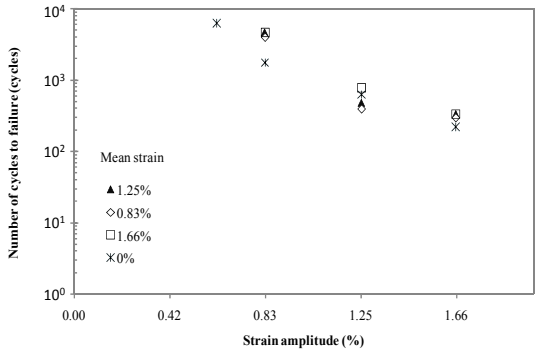

Fig. 7
Changes in the fatigue lives of the specimens to the strain amplitude for CK45 steel.

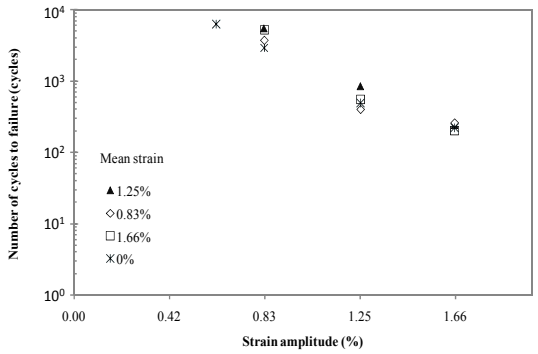

Fig. 8
Changes in the fatigue lives of the specimens to the strain amplitude for SS316 stainless steel.

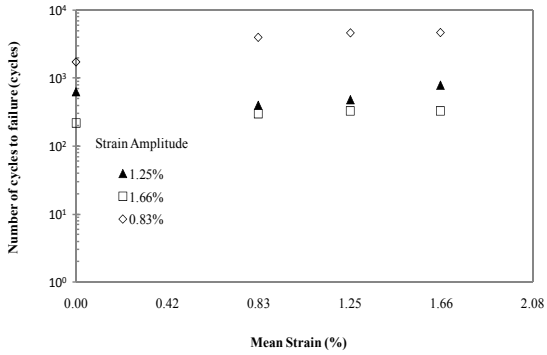

Fig. 9
Changes in the fatigue lives of the specimens to the mean strain for CK45 steel.

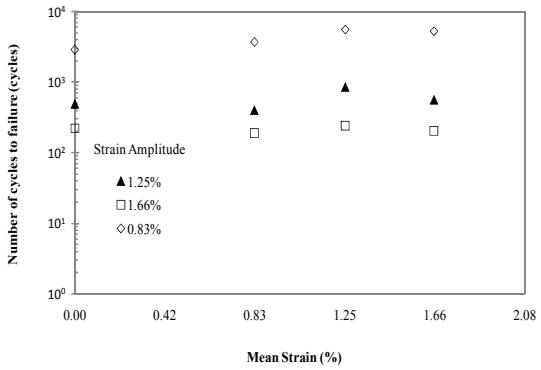

Fig. 10
Changes in the fatigue lives of the specimens to the mean strain for SS316 stainless steel.

3.2.1 Predicting the fatigue life based on damage parameters

Different varieties of models can be used to predict the fatigue life. These models can be based on energy or strain/stress criteria. The most common strain/stress based is SWT model. This model employs a series of material specific constants to connect the fatigue life to the strain or stress in cyclic loading with mean stress or mean strain. The SWT parameter [5] is given in Eq (1).

$$\sigma_{ar} = \sqrt{\sigma_{\max}\sigma_a} = \sigma_{\max}\sqrt{\frac{1-R}{2}} = \sigma_a\sqrt{\frac{2}{1-R}} \tag{1}$$

where, σ_{ar} is the equivalent fully reversed stress amplitude, σ_{max} is the maximum stress, σ_a is the stress amplitude and R is the stress ratio ($R=\sigma_{min}/\sigma_{max}$). Based on Basquin's equation [18], stress-life curve is assumed to follow power relationship (Eq. (2)).

$$\sigma_a = \sigma'_f(2N_f)^b \tag{2}$$

where N_f is cycles to failure and b, σ_f' are fitting constants which are determined from tests under zero mean stress, also called fully reversed tests. In short fatigue life analysis, the strain amplitude ε_a is used to develop fatigue-life curves by relating strain amplitude to the number of cycles to failure which is called Coffin-Manson equation [19,20].

$$\frac{\Delta\varepsilon}{2} = \varepsilon_a = \frac{\Delta\varepsilon^e}{2} + \frac{\Delta\varepsilon^p}{2} = \frac{\sigma'_f}{E}\left(2N_f\right)^b + \varepsilon'_f\left(2N_f\right)^c \tag{3}$$

where, $\Delta\varepsilon^p$ and $\Delta\varepsilon^e$ are plastic and elastic strain range, ε_a is the strain amplitude, E is the elastic modulus, b and c are empirical constants and σ'_f and ε'_f are the fatigue strength and the fatigue ductility, respectively. An extension of the SWT parameter is defined by replacing σ_a in Eq. (1) with ε_a .

$$\sigma_{max}\varepsilon_a = \sigma_{max}\frac{\Delta\varepsilon}{2} = \frac{(\sigma'_f)^2}{E}\left(2N_f\right)^{2b} + \varepsilon'_f\sigma'_f\left(2N_f\right)^{b+c} \tag{4}$$

where $\sigma_{max}= \sigma_{m+} \sigma_a$ is the stable maximum stress, $\Delta\varepsilon$ is the strain range, $2N_f$ is the number of reversals to failure. In addition, the term $\sigma_{max}\,\varepsilon_a$ is referred to SWT parameter.

In the energy method, the fatigue life of the material is associated with the strain energy generated over the course of loading cycles until the failure. In a cyclic loading with a constant amplitude, the strain energy in each cycle is equal to the sum of elastic strain energy and plastic strain energy, shown with Eq. (5) and Eq. (6) [8,10,21].

$$\Delta W = \Delta W_e + \Delta W_p \tag{5}$$

$$\Delta W = \oint_{cycle} \sigma d\varepsilon_e + \oint_{cycle} \sigma d\varepsilon_p \tag{6}$$

where, ΔW, ΔW_e, ΔW_p, ε_e, and ε_p are, in turn, the total strain energy, elastic strain energy, plastic strain energy, elastic strain, and plastic strain. The elastic and plastic strains can be written as following, assuming that strain cyclic curves are in form of Ramberg-Osgood [22] :

$$\varepsilon_e = \frac{\sigma}{E} \tag{7}$$

$$\varepsilon_p = \left(\frac{\sigma}{k'}\right)^{1/n'} \tag{8}$$

where, n' and k' are constants of the material. Moreover, Eq. (9), given by Halford [8] , and Golos and Ellyin [10] , indicates the relationship between hysteresis strain energy and the number of reversals up to the failure.

$$\Delta W = A\left(2N_f\right)^{\alpha} \tag{9}$$

In this Equation, A and α are the constants of the material denote, in turn, energy absorption capacity of the material and fatigue exponent.

According to Eq. (6), the hysteresis strain energy generated in each cycle equates the enclosed area of the hysteresis loop obtained from experimental strain-control tests. In this study, the energy damage parameter ΔW_p and the SWT damage parameter were used to predict fatigue life under strain control loading with mean strain. In addition, the two model were compared with experimental results. Fig. 11 shows a graphical illumination of the two damage parameter. As can be seen, the magnitude of the SWT and energy damage parameters are equal to the enclosed areas within the curve OABCO and DBEFGHD, respectively. The calculated results for ΔW_p and SWT damage parameters are listed in Table 2. It should be noted that the hysteresis loop at half fatigue life was considered to obtain the damage parameters for each test in a steady state.

Finally, by plotting the damage parameters versus fatigue life for fully reversed cyclic fatigue tests and by fitting a curve the two following equations for predicting fatigue life curve based on SWT and energy damage parameter ΔW_p for CK45 steel were found.

$$\sigma_{max}\varepsilon_a = 95.25\left(2N_f\right)^{-0.446} \tag{10}$$

$$\Delta W_p = 246.42\left(2N_f\right)^{-0.516} \tag{11}$$

Similar procedure was carried out for SS316 stainless steel and two following equations for predicting fatigue life curve based on SWT and energy damage parameter ΔW_p were found.

$$\sigma_{max}\varepsilon_a = 80.12\left(2N_f\right)^{-0.411} \tag{12}$$

$$\Delta W_p = 306.23\left(2N_f\right)^{-0.55} \tag{13}$$

To investigate the accuracy of the obtained equations, the number of experimental and predicted reversals to failure by two equations for CK45 steel specimens are plotted in Figs. 12 and 13. From Fig. 12 it can be seen that the energy damage parameter ΔW_p appears to be accurate and all points fall inside the life factor 2 scatter bands. From Fig. 13, it can be seen that for SWT damage parameter a few points lie outside the bands and the points have a relatively larger scatter in comparison to the energy damage parameter. Hence, it can be concluded that the energy damage parameter provides more accurate prediction of fatigue life for CK45 steel under strain-control cyclic loading. Figs. 14 and 15 show comparison of experimental and predicted fatigue life by using energy and SWT damage parameters for SS316 stainless steel. As can be seen, for both damage parameters, all data points fall within the life factor 2 scatter bands. Although for a few experiments the data points for SWT damage parameter (Fig. 15) fall near the scatter bands, both damage parameters present a relatively good correlation between the predicted and the experimental fatigue lives.

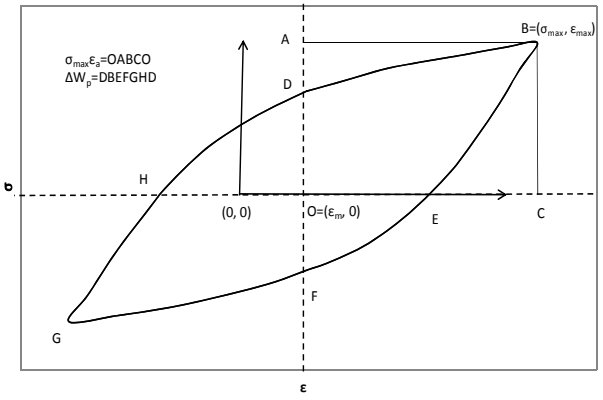

Fig. 11
Graphical illumination of the SWT and energy damage parameter.

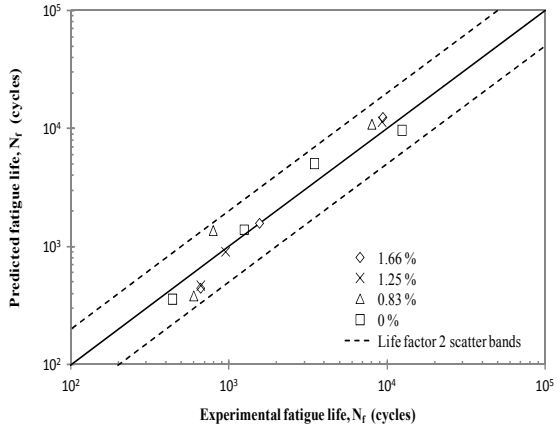

Fig. 12
Comparison of experimental and predicted fatigue lives based on energy fatigue damage parameter, ΔW_p for CK45 steel.

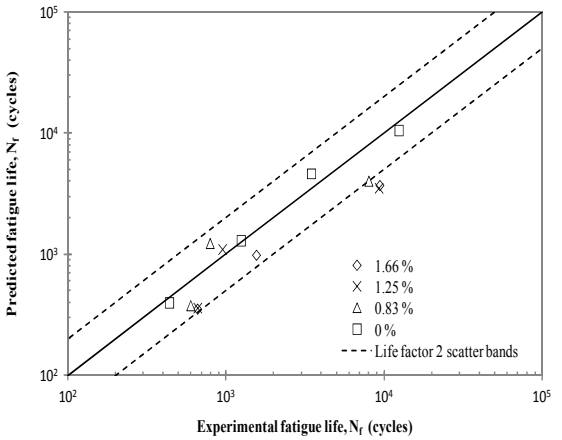

Fig. 13
Comparison of experimental and predicted fatigue lives based on SWT fatigue damage parameter, $\sigma_{max}\ \varepsilon_a$ for CK45 steel.

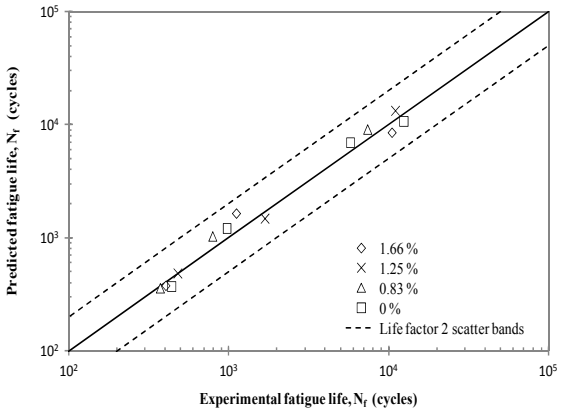

Fig. 14
Comparison of experimental and predicted fatigue lives based on energy fatigue damage parameter, ΔW_p for SS316 stainless steel.

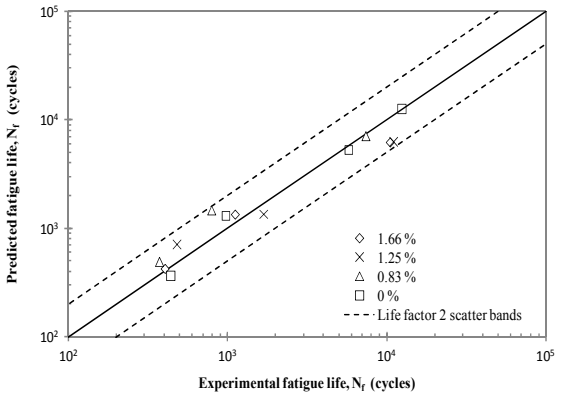

Fig. 15
Comparison of experimental and predicted fatigue lives based on SWT fatigue damage parameter, $\sigma_{max}\ \varepsilon_a$ for SS316 stainless steel.

3.2.2 Prediction errors

In order to clarify the accuracy of the parameters more precisely, the standard deviation of the prediction errors is calculated for both materials by using Eq. (14)

$$\prod = \sqrt{\sum_{i=1}^{n} \frac{(\Delta_i - \bar{\Delta})^2}{n-1}} \tag{14}$$

Table 3
Calculated results of the standard deviation of the prediction errors for two damage parameters

Material	$\prod$ for ΔW_p	$\prod$ for SWT
CK45	598	1174
SS316	510	876

where Δ is the difference between the predicted and experimental fatigue life, $\overline{\Delta}$ is the average value of Δ_i and n is the number of experiments. The calculated results for $\prod$ are listed in Table 3. for both damage parameters and materials. From Table 3. it can be seen that the value of the standard deviation of the prediction errors for energy damage parameter, ΔW_p is less than the value of that for SWT damage parameter for both materials. Therefore, this indicates that the energy damage parameter, ΔW_p provides more accurate life prediction than the SWT damage parameter for both CK45 steel and SS316 stainless steel.

4 CONCLUSIONS

Based on the experimental results presented in this work, it could be concluded that:

1. The cyclic softening/hardening behavior of the both materials is related to the strain amplitudes. For CK45 steel specimens, full softening behavior is seen for small strain amplitudes. This behavior is in hardening form for large strains in initial cycles (about 15 cycles), which then turns into softening behavior again. After about 200 cycles, this behavior once more becomes softening till failure. For SS316 stainless steel the stress amplitude increases with a rapid rate at initial cycles and after that the material presents apparent cyclic softening behavior. The material shows a relatively higher softening behavior when the strain amplitude is relatively larger.
2. The fatigue life decreased significantly as the strain amplitude was increased in constant mean strain for both materials. In addition, for CK45 steel, increased mean strain slightly increase fatigue life and for SS316 stainless steel, the fatigue lives are slightly increased by increasing the mean strain till mean strain of 1.25% and after that the fatigue lives are slightly begun to decrease. In general, it can be concluded that for the loading range which is presented in this study, the fatigue life is highly affected by the strain amplitude and the effect of mean strain on it is almost ignorable.
3. The energy damage parameter provides more accurate prediction of fatigue life for CK45 steel and SS316 stainless steel under strain-control cyclic loading in comparison to SWT damage parameter.

REFERENCES

[1] Yang X., 2005, Low cycle fatigue and cyclic stress ratcheting failure behavior of carbon steel 45 under uniaxial cyclic loading, *International Journal of Fatigue* **27**: 1124-1132.
[2] Date S., Ishikawa H., Otani T., Takahashi Y., 2008, Effect of ratcheting deformation on fatigue and creep-fatigue life of 316FR stainless steel, *Nuclear Engineering and Design* **328**: 336-346.
[3] You B-R., Lee S-B., 1996, A critical review on multiaxial fatigue assessments of materials, *International Journal of Fatigue* **18**(4): 253-344.
[4] Jahed H., Farahani A.V., Noban M., Khalaji I., 2007, An energy based fatigue life assessment model for various metallic materials under proportional and non-proportional loading conditions, *International Journal of Fatigue* **29**: 647-655.
[5] Smith R.N., Watson P., Topper T.H., 1970, A stress-strain function for the fatigue of metal, *Journal of Material, JMLSA* **5**(4): 767-778.
[6] Lorenzo F., Laird C., 1984, A new approach to predicting fatigue life behavior under the action of mean stresses, *Material Science and Engineering* **62**(2): 205-210.
[7] Koh S.K., Stephens R.I., 1991, Mean stress effects on low cycle fatigue for a high strength steel, *Fatigue & Fracture of Engineering Materials & Structures* **14**(4): 413-428.
[8] Halford G.J., 1966, The energy required for fatigue, *Journal of Materials* **1**(1): 3-18.
[9] Kujawski D., Ellyin F., 1995, A unified approach to mean stress effect on fatigue threshold conditions, *International Journal of Fatigue* **12**(2): 101-106.
[10] Golos K., Ellyin F.A., 1988, A total strain energy density theory for cumulative fatigue damage, *Journal of Pressure Vessel Technology* **110**(1): 36-41.

[11] Sugiura K., Chang K.C., 1991, Evaluation of low-cycle fatigue strength of structural metal, *Journal of Engineering Mechanics (ASCE)* **117**(10): 2373-2383.
[12] Dutta A., Dhar S., Acharyya S.K., 2010, Characterization of SS316 in low-cycle fatigue loading, *Journal of Materials Science* **45**(7): 1782-1789.
[13] Callaghan M.D., Humphries S.R., Law M., Ho M., Bendeich P., Li H., Yeung W.Y., 2010, Energy-based approach for the evaluation of low cycle fatigue behavior of 2.25cr-1 Mo steel at elevated temperature, *Materials Science & Engineering* **527** (21-22): 5619-23.
[14] Lv F., Yang F., Li S.X., Zhang Z.F., 2011, Effect of hysteresis energy and mean stress on low-cycle fatigue behaviors of and extruded magnesium alloy, *Scripta Materialia* **65**(1): 53-56.
[15] Abdalla J.A., Hawileh R.A., Oudah, F., Abdelrahman K., 2009, Energy-based prediction of low-cycle fatigue life of BS 460B and BS B500B steel bars, *Material & Design* **30**: 4405-4413.
[16] Gloanec A.I., Milani T., Henaff G., 2010, Impact of microstructure, temperature and strain ratio on energy-based low-cycle fatigue life prediction models for TiAl alloys, *International Journal of Fatigue* **32**(7): 1015-1021.
[17] Yunrong L.U., Chongxiang H.U., Li G., Qingyuan W., 2012, Energy-based prediction of low-cycle fatigue life of high-strength structural steel, *International Journal of Iron and Steel Research* **19**(10): 47-53.
[18] Basquin O.H., 1910, The exponential law of endurance tests, *American Society for Testing Materials* **10**: 625-630.
[19] Coffin L.F., 1954, A study of the effects of cyclic thermal stresses on a ductile metal, *Transactions of the ASME* **76**: 931-950.
[20] Manson S.S., 1953, Behavior of materials under condition of thermal stress, *Heat Transfer Symposium, University of Michigan Engineering Research Institute*, MI, USA.
[21] Tchankov D.S, Vesselinov K.V., 1998, Fatigue life prediction under random loading using total hysteresis energy, *International Journal of Pressure Vessels and Piping* **75**: 955-960.
[22] Lagoda T., 2001, Energy models for fatigue life estimation under uniaxial random loading part I: the model elaboration, *International Journal of Fatigue* **23**: 467-480.